ACS Catalysis

Letter

pubs.acs.org/acscatalysis

100° Temperature Reduction of Wet Methane Combustion: Highly Active Pd–Ni/Al_2O_3 Catalyst versus Pd/$NiAl_2O_4$

Jing Shen, Robert E. Hayes, Xiaoxing Wu, and Natalia Semagina*

Department of Chemical and Material Engineering, University of Alberta, 9107-116 Street, Edmonton, Alberta T6G 2 V4, Canada

Supporting Information

ABSTRACT: The crucial role of Ni mode addition to Pd catalysts for low-temperature wet methane combustion is addressed, resulting in excellent performance of ultralow-Ni-containing catalysts versus inactive nickel–alumina spinel. Traditional impregnation–calcination and colloidal techniques of bimetallic catalyst preparation yield monometallic Pd particles on a binary $NiAl_2O_4$ support and Pd and Ni nanoparticles on the parent Al_2O_3 support, respectively. The catalyst is potentially valuable for natural gas catalytic combustion technologies because it decreases the required temperature for complete methane combustion in 5% water presence in the feed by 100 degrees versus monometallic Pd.

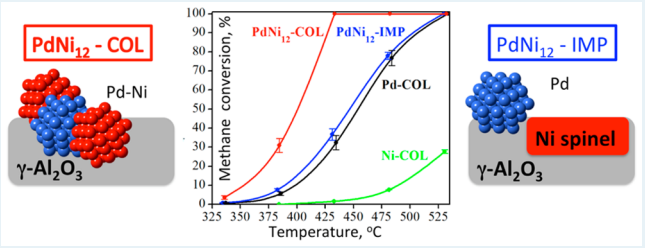

KEYWORDS: *palladium, nickel, spinel, bimetallic nanoparticles, methane combustion*

Recently, revived interest in catalytic methane combustion has been brought about by the increasing demand in natural-gas operated vehicles, heating devices, and gas turbines.[1,2] The release of methane is an environmental concern because it is the second most significant greenhouse gas, with a global warming potential 23 times higher than that of CO_2. The use of heterogeneous catalysts allows complete methane oxidation at relatively low temperatures, as compared with thermal combustion. Alumina-supported palladium catalysts are generally accepted as the most active CH_4 oxidation catalysts and have been extensively studied, including methods to improve Pd nanoparticle stability toward sintering.[1−3] Methane combustion catalysts must achieve an ignition temperature of 200–300 °C[1] and complete oxidation temperature below 500–550 °C;[3] however, maintaining low-temperature Pd stability in the presence of water is challenging[4] because inactive palladium hydroxide could be retained at temperatures up to 450 °C.[3,5] One of the proposed solutions to improve the hydrothermal stability of Pd/Al_2O_3 catalysts is to use metal oxide additives in the alumina support.[6−11]

Introducing a second metal component into a heterogeneous catalyst support has been widely accepted as one of the ways to increase activity, selectivity, and stability of the deposited catalytic metal nanoparticles.[12] For the catalysts to be stable in a high-temperature oxidizing atmosphere, the least lattice mismatch between the supported Pd or Pt nanoparticles and spinels of nickel[6] or magnesium,[12] respectively, has been shown to be responsible for the enhanced nanoparticle stability toward sintering. This approach, however, requires high amounts of the second metal (often more than one-half of the support weight), and it brings complexity to the large-scale support production and increases the material's price. Nickel oxide-promoted alumina has received particular attention because of improved Pd catalyst stability in methane combustion, including in the presence of water. The enhancement is ascribed to the Pd dispersion stabilizing effect by $NiAl_2O_4$ spinel,[6−8] whereas some observations claim the opposite effect because of the lowered surface area of alumina support by Ni.[13] The Ni content in the alumina support must be extremely high to achieve a notable improvement in the Pd activity. For example, a 35 °C reduction in the 90% methane conversion temperature was obtained by adding 36:1 NiO to the alumina support.[7] Several attempts have been made to validate experimentally the effect of alloying Pd and Ni with similar loadings and ensure their close contact, but because the catalysts were prepared by conventional coprecipitation or impregnation, Ni was consumed in spinel formation or did not yield a noticeable improvement in the catalytic performance.[13−15] Such traditional methods for bimetallic catalyst synthesis are known to be inefficient in providing nanoparticle structure control.[16]

In this study, we report a successful preparation of modified Pd catalysts with ultralow Ni content (12:1 molar ratio of Ni to Pd) yielding PdO–NiO bimetallic catalyst, which allowed methane combustion at 430 °C in the presence of 5 mol % water in the feed. The Pd–Ni particles were prepared before deposition on the support by a colloidal chemistry technique with poly(vinylpyrrolidone) (PVP) as a stabilizer. The method of Ni incorporation is shown to be paramount: when the same Ni amount was introduced via traditional support impregnation, it was consumed into spinel formation and did not show any improvement in catalytic activity versus monometallic Pd

Received: January 13, 2015
Revised: April 6, 2015
Published: April 7, 2015

DOI: 10.1021/acscatal.5b00060
ACS Catal. 2015, 5, 2916–2920

catalyst. The diagram depicting the two approaches in the catalyst preparation is provided in Figure 1.

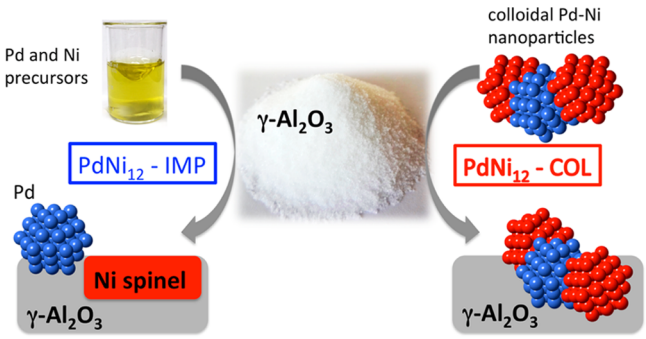

Figure 1. Schematic of bimetallic catalyst preparation via traditional impregnation–calcination ($PdNi_{12}$-IMP) and colloidal techniques ($PdNi_{12}$-COL), resulting in monometallic particles on a binary support (left) and Pd and Ni nanoparticles on the parent support (right).

Colloidal Pd-COL, Ni-COL and $PdNi_{12}$-COL nanoparticles were synthesized by the reduction of $PdCl_2$ or $Ni(NO_3)_2{\cdot}6H_2O$ precursors in alcohol media in the presence of poly-(vinylpyrrolidone) (PVP), followed by deposition on γ-Al_2O_3 support. The metal loadings were found by neutron activation analysis as 0.190 wt % Ni and 0.029 wt % Pd, with the 12-to-1 Ni-to-Pd molar ratio. The notation $PdNi_{12}$-COL only indicates the overall catalyst molar composition, not the phase composition. $PdNi_{12}$-IMP catalyst was prepared by incipient wetness impregnation of the support with an aqueous solution of the same precursors. The Pd-COL, $PdNi_{12}$-IMP, and Ni-COL catalysts were prepared with the same loadings for fair comparison (0.029 wt % Pd and 0.190 wt % Ni). All catalysts were calcined under static air at 550 °C for 16 h. The catalyst synthesis details can be found in the Supporting Information.

Catalytic wet methane combustion was conducted in the presence of 5 mol % of water in the feed (4100 ppm of CH_4 in N_2 and air mixture) at 1.1 barg pressure. All experiments were performed with the same total catalyst amount in the reactor with the same loadings corresponding to 1.2 mg Pd or 7.6 mg Ni. Ignition and extinction curves were obtained between 200 and 550 °C. First, two ignition–extinction experiments (without and with 5 mol % water, respectively) were performed to precondition the catalyst, followed by the hydrothermal aging in the wet methane/air feed by increasing the reaction temperature to 550 °C and then cooling the reactor to the temperature that gives ~50% CH_4 conversion. The high–low temperature cycling was repeated eight times (about 22 h). After the cycling was completed, the reactor temperature was then held at the selected temperature for another 18 h. Finally, a third ignition–extinction test (with 5 mol % water) was performed to check the activity of the aged catalyst. These data are reported in Figure 2. Further experimental details are available in the Supporting Information.

As seen from Figure 2, the use of colloidal $PdNi_{12}$-COL catalyst lowers the complete methane combustion temperature by ~100 °C as compared with monometallic Pd (Pd-COL) at the same Pd loading in the reactor and in the supported catalysts. Remarkably, Ni addition by coimpregnation with metal precursors ($PdNi_{12}$–IMP) did not show any improvement in the catalytic activity versus Pd. The same trend was observed during the hydrothermal aging of the three catalysts:

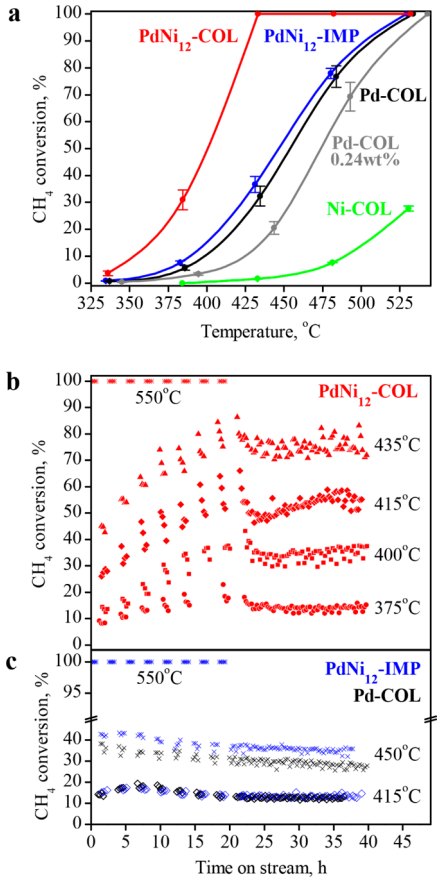

Figure 2. Wet methane combustion, 4100 ppm methane, 5 mol % water, 1.1 barg pressure, 1.2 mg Pd, 7.6 mg Ni (0.029 wt % Pd and 0.190 wt % Ni loading in relevant catalysts, except for the 0.24 wt % Pd catalyst): (a) ignition–extinction curves after 40 h of time on-stream (no hysteresis was observed), (b, c) hydrothermal aging. Error bars represent one standard deviation from average for all ignition–extinction curves (b, c) after 40 h on-stream.

both Pd-COL and $PdNi_{12}$-IMP showed 10–40% conversions in the temperature range of 415 to 450 °C, and the $PdNi_{12}$–COL catalyst allowed 80% conversion at 435 °C. The $PdNi_{12}$-COL catalyst did not deactivate for at least 40 h on-stream at temperatures of 375–435 °C. This temperature window indicates the outstanding colloidal catalyst stability in the presence of water: the effect of water on Pd catalysts is known to be significant at lower temperatures and almost negligible at 450 °C and above.[5] Colloidal monometallic nickel catalyst (Ni-COL) displayed the least activity (38% conversion at 550 °C at the same loading as in the bimetallic catalysts).

Chlorine-containing Pd precursor was used for the catalyst preparation, and it can be poisonous for the catalytic activity,[3] so its content was verified via X-ray photoelectron spectroscopy (XPS). The $PdNi_{12}$-COL catalyst contains a negligible amount of Cl (0.1 wt %) after calcination at 550 °C for 16 h, which is likely due to washing of the preformed nanoparticles. The $PdNi_{12}$-IMP catalyst had quite a significant chlorine content (0.7 wt %) after the calcination, but it was below the detection limit for the sample after the hydrothermal aging for 40 h, most likely because of the cleaning effect of a steam–air mixture. To confirm that the lower activity of the $PdNi_{12}$-IMP catalyst is not due to the chlorine presence, another impregnated catalyst was prepared with palladium acetate and tested at 450 °C: the catalytic results were the same (<3% conversion difference) as

DOI: 10.1021/acscatal.5b00060
ACS Catal. 2015, 5, 2916–2920

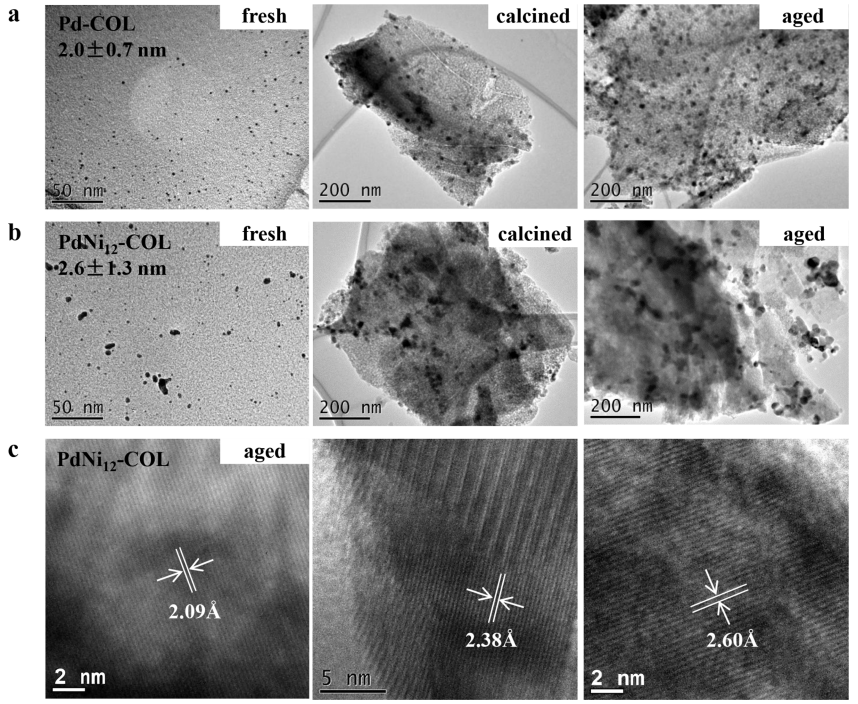

Figure 3. TEM images of Pd-COL (a) and $PdNi_{12}$-COL (b, c) catalysts: nanoparticles before deposition on the support ("fresh"); after deposition and calcination for 16 h at 550 °C ("calcined"), and after hydrothermal aging (methane combustion) for 40 h ("aged").

those for the $PdNi_{12}$-IMP catalyst prepared from palladium chloride. Thus, the chlorine effect can be considered negligible.

Because bimetallic catalysts may show improved stability against sintering,[17] the addition of Ni to Pd during the colloidal synthesis could potentially prevent growth of Pd nanoparticles known to occur at high-temperature oxidation processes. The ability to control collective properties of nanoparticles is crucial for their stable performance.[18] Herein, the as-prepared nanoparticle sizes are comparable for both catalysts in the range of 2−3 nm, as seen from their transmission electron microscopy (TEM) images (Figure 3), being on the higher side for the $PdNi_{12}$-COL sample. Both Pd-COL and $PdNi_{12}$-COL catalysts exhibited similar sintering behavior after calcination and hydrothermal aging. The higher degree of agglomeration for the bimetallic catalyst is due to the overall higher metal loading (0.03 wt % Pd in Pd-COL and 0.03 wt % Pd to 0.19 wt % Ni in $PdNi_{12}$-COL). Thus, nickel addition does not noticeably improve the nanoparticle stability against sintering.

A plausible explanation of the enhanced activity of the bimetallic colloidal catalyst could be related to its enhanced agglomeration versus the monometallic Pd-COL. Indeed, it is known that turnover frequency of Pd catalysts in methane combustion increases as high as 2 orders of magnitude with decreasing dispersion.[19−22] To verify this hypothesis, we prepared a higher loading Pd-COL 0.24 wt % catalyst so that the catalyst approaches the bimetallic catalyst by the metal(s) weight loading. As found by CO chemisorption, after 16 h calcination at 550 °C, the Pd dispersion in 0.24 wt % Pd-COL catalyst is 10% (13 nm particle size) versus 28% (4.8 nm particle size) for the 0.03 wt % Pd-COL catalyst. TEM of the higher-loading Pd catalyst (see the Supporting Information, Figure S1) confirmed the excessive sintering and resembled the image for the $PdNi_{12}$-COL catalyst (Figure 3b). However, when tested in the wet methane combustion with the same Pd amount in the reactor (Figure 2a), the higher-loading catalyst not only was much less active than the $PdNi_{12}$−COL catalyst, but also exhibited lower activity as opposed to the lower-loading Pd-COL catalyst. Thus, the activity enhancement effect for the $PdNi_{12}$-COL catalyst cannot be explained by a higher overall metal loading and decreased dispersion.

To compare our findings with the literature data, we performed dry methane combustion and evaluated the TOF under different conditions at 254 °C as 0.008 s^{-1} (for the 0.24 wt % Pd-COL catalyst with 10% Pd dispersion, 13 nm particle size; the TOF is for the third ignition−extinction curve after 40 h on-stream). Using the activation energy value of 117 kJ/mol,[22] the extrapolated exemplary reported TOFs for Pd/Al_2O_3 catalysts at 254 °C are 0.0082 s^{-1} (2.2 wt % Pd loading, 14 nm particle size)[20] and are in the range of 0.0017 s^{-1} (0.46 wt % Pd loading, 35% Pd dispersion) to 0.094 s^{-1} (2.3 wt % Pd loading, 10% Pd dispersion).[22] Our 0.24 wt % Pd-COL catalyst prepared via the colloidal technique showed 14 times higher TOF than the reported impregnated Pd catalyst with the same loading (0.2 wt %).[22] The enhancement is likely due to the lower Pd dispersion in the colloidal catalyst (10% versus 84% for the reported catalyst) because the 2 nm Pd nanoparticles were formed before deposition on the support.

To understand the observed differences between the colloidal $PdNi_{12}$−COL and impregnated $PdNi_{12}$-IMP catalysts, the materials were subjected to temperature-programmed reduction (TPR) and revealed distinctly different profiles (Figure 4a). The Pd-COL catalyst shows only a hydrogen evolution peak below 100 °C, indicative of hydride decomposition.[23] The reduction of the $PdNi_{12}$-COL catalyst occurs at 383 °C, which can be assigned to the reduction of NiO.[24] Although the TPR test for the $PdNi_{12}$-COL catalyst was performed with the same Pd loading as the monometallic Pd-COL sample, the negative hydrogen evolution peak corresponding to Pd disappeared in the $PdNi_{12}$-COL catalyst; this could be an indication of Ni-Pd interactions in the latter. The

DOI: 10.1021/acscatal.5b00060
ACS Catal. 2015, 5, 2916−2920

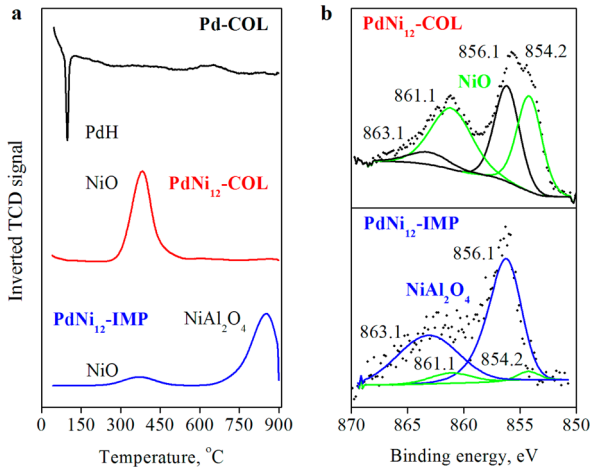

Figure 4. Spinel and NiO phase formation in the catalysts after calcination at 550 °C, 16 h: (a) temperature-programmed reduction profiles with the same loadings of Pd and Ni in H_2/Ar flow (negative inverted TCD signal indicates hydrogen evolution); (b) high-resolution X-ray photoelectron spectra of Ni $2p_{3/2}$.

$PdNi_{12}$-IMP catalyst showed only a small broad peak at 383 °C and a strong reduction peak with a maximum of 850 °C, which is characteristic of $NiAl_2O_4$ spinels for catalysts prepared by coimpregnation of Ni and Pd precursors on alumina support.[6,24] Thus, as TPR shows, the method of Pd−Ni catalyst preparation is crucial for the final catalyst structure: no spinel formation occurred when nanoparticles were formed in the absence of alumina.

The XPS analysis of the calcined samples confirmed the TPR findings (Figure 4b): the Ni $3p_{3/2}$ peaks from NiO (main 854.2 eV and its satellite 861.1 eV[25]) are insignificant for the impregnated sample, as opposed to the colloidal catalyst. The 856.1 eV peak may be ascribed to both a NiO shoulder and spinel $NiAl_2O_4$, with a satellite at 863.1 eV,[25] but in the impregnated sample, the two peaks represent virtually all present Ni states, without NiO at 854.2 eV, indicating that nickel in the impregnated sample is consumed in the spinel formation, in agreement with the TPR data. Pd $3d_{5/2}$ peaks in all three Pd-COL, $PdNi_{12}$-COL, and $PdNi_{12}$-IMP samples (Supporting Information, Figure S2) could be assigned to PdO (336.5 eV) and PdO_x (337.4 eV). The peak ratios of PdO/PdO_x are identical for the colloidal mono- and bimetallic catalysts, but the impregnated catalyst exhibited a significantly lower value. Smaller Pd crystallites, such as in the impregnated sample, are known to be oxidized to a larger extent versus larger particles, which leads to the decreased catalytic activity,[22] in agreement with our data. No shifts in Pd binding energy because of possible alloying with Ni were observed.

The $PdNi_{12}$-COL catalyst was further investigated via high-resolution HR-TEM after the hydrothermal aging to gain more insight into the possible alloy structure of Ni−Pd bimetallic nanoparticles (Figure 3c). The lattice spacings of 0.209, 0.241, and 0.263 nm are characteristic of cubic NiO (200), NiO (111), and tetragonal PdO (101), respectively. An XRD pattern (Supporting Information, Figure S3) also shows the presence of tetragonal PdO and cubic NiO phases, with no shifts that could suggest the intrinsic Pd−Ni alloy structure. Although Pd and Ni form alloys of unlimited mutual miscibility, a similar segregation of Pd and Ni oxides supported on alumina were observed in their temperature-programmed oxidation and reduction study.[26] Nevertheless, the catalytic results are indicative of the interactions between the PdO and NiO phases in the $PdNi_{12}$−COL catalyst. The nature of such interactions is currently under study, with a hypothesis that NiO particles participate in the redox Mars and van Krevelen mechanism,[27,28] when reduced Pd is reoxidized with oxygen from NiO and Al_2O_3. The NiO presence may become beneficial in the wet combustion because water was suggested to decrease the oxygen exchange with the support.[27]

Therefore, when the bimetallic catalyst was prepared by the traditional impregnation method, Ni precursor reacted with alumina support and formed inactive $NiAl_2O_4$ spinel during high temperature treatment, which explains the lack of improvement in methane oxidation activity as compared with the monometallic Pd. Previous studies of impregnated Pd−Ni catalysts on alumina support also reported the formation of the $NiAl_2O_4$ spinel phase and a small amount of NiO with no improvement of Pd performance in CH_4 oxidation.[13,15] The improved performance was noticed only if a very high Ni content was employed (36:1 NiO/Al_2O_3).[7]

Our study demonstrates the dramatic importance of the synthetic strategy for effective promotion of supported metal nanoparticles by a low-quantity metal promoter. In the present state, however, the developed bimetallic catalyst cannot be applied for realistic space velocities because of the low Pd loading, and bottom-up strategies must be developed to increase the loading of preformed Pd−Ni nanoparticles on the support.[2] The conversions reported in Figure 2 for the $PdNi_{12}$-COL, $PdNi_{12}$-IMP, and Pd-COL were measured for the same space velocities for fair comparison. The value of our findings is in the dramatically increased activity of the Pd catalyst in the presence of water, caused by Ni addition at the lowest reported in literature weight ratio of Ni to Pd (6.5-to-1 versus, for example, 70, as was shown previously for only a 35° temperature reduction[7]). In general, the results indicate that it is possible to reevaluate the effect of binary supports on supported metal nanoparticles' catalytic performance by introducing a relevant support component into the alloy (or segregated alloy) structure with the supported nanoparticles, thus reducing the support cost and localizing the desired effects on the catalyst surface.

■ ASSOCIATED CONTENT

Supporting Information

The following file is available free of charge on the ACS Publications website at DOI: 10.1021/acscatal.5b00060.

Experimental details of catalyst synthesis, characterization and catalytic tests; supporting figures for TEM, XPS, and XRD of selected samples (PDF)

■ AUTHOR INFORMATION

Corresponding Author

*E-mail: Semagina@ualberta.ca.

Notes

The authors declare no competing financial interests.

■ ACKNOWLEDGMENTS

Financial support from NSERC − Strategic Program Grant STPGP 430108−12 is acknowledged. We thank Dimitre Karpuzov for the XPS analysis, Shiraz Merali for XRD analysis, and Becquerel Laboratory of Maxxam Analytics (Ontario, Canada) for NAA analysis.

DOI: 10.1021/acscatal.5b00060
ACS Catal. 2015, 5, 2916−2920

REFERENCES

(1) Centi, G. *J. Mol. Catal. A: Chem.* **2001**, *173*, 287−312.
(2) Cargnello, M.; Delgano Jaen, J. J.; Hernandez Garrido, J. C.; Bakhmutsy, K.; Montini, T.; Calcino Gamez, J. J.; Gorte, R. J.; Fornasiero, P. *Science* **2012**, *337*, 713−717.
(3) Gelin, P.; Primet, M. *Appl. Catal., B* **2002**, *39*, 1−37.
(4) Farrauto, R. J. *Science* **2012**, *337*, 659−660.
(5) Burch, R.; Urbano, F. J.; Loader, P. K. *Appl. Catal., A* **1995**, *123*, 173−184.
(6) Liu, Y.; Wang, S.; Sun, T.; Gao, D.; Zhang, C.; Wang, S. *Appl. Catal., B* **2012**, *119*−*120*, 321−328.
(7) Widjaja, H.; Sekizawa, K.; Eguchi, K.; Arai, H. *Catal. Today* **1999**, *47*, 95−101.
(8) Yue, B.; Zhou, R.; Wang, Y.; Zheng, X. *Appl. Surf. Sci.* **2006**, *252*, 5820−5828.
(9) Sekizawa, K.; Eguchi, K.; Widjaja, H.; Machida, M.; Arai, H. *Catal. Today* **1996**, *28*, 245−250.
(10) Widjaja, H.; Sekizawa, K.; Eguchi, K.; Arai, H. *Catal. Today* **1997**, *35*, 197−202.
(11) Yang, L.; Shi, C.; He, X.; Cai, J. *Appl. Catal., B* **2002**, *38*, 117−125.
(12) Li, W. Z.; Kovarik, L.; Mei, D.; Liu, J.; Wang, Y.; Peden, C. H. F. *Nat. Commun.* **2013**, *4*, 2481.
(13) Pan, X.; Zhang, Y.; Miao, Z.; Yang, X. *J. Energy Chem.* **2013**, *22*, 610−616.
(14) Pan, X.; Zhang, Y.; Zhang, B.; Miao, Z.; Wu, T.; Yang, X. *Chem. Res. Chin. Univ.* **2013**, *29*, 952−955.
(15) Persson, K.; Ersson, A.; Jansson, K.; Iverlund, N.; Jaras, S. *J. Catal.* **2005**, *231*, 139−150.
(16) Lu, J.; Low, K. B.; Lei, Y.; Libera, J. A.; Nicholls, A.; Stair, P. C.; Elam, J. W. *Nat. Commun.* **2014**, *5*, 3264.
(17) Cao, A.; Veser, G. *Nat. Mater.* **2010**, *9*, 75−81.
(18) Prietro, G.; Zecevic, J.; Friedrich, H.; de Jong, K. P.; de Jong, P. E. *Nat. Mater.* **2012**, *12*, 34−39.
(19) Muller, C. A.; Maciejewski, M.; Koeppel, R.A.l; Baiker, A. *J. Catal.* **1997**, *166*, 36−43.
(20) Roth, D.; Gelin, P.; Kaddouri, A.; Garbowski, E.; Primet, M.; Tena, E. *Catal. Today* **2006**, *112*, 134−138.
(21) Fujimoto, K.; Ribeiro, F. H.; Avalos-Borja, M.; Iglesia, E. *J. Catal.* **1998**, *179*, 431−442.
(22) Hicks, R. F.; Qi, H.; Young, M. L.; Lee, R. G. *J. Catal.* **1990**, *122*, 280−294.
(23) Shen, J.; Semagina, N. *ACS Catal.* **2014**, *4*, 268−279.
(24) Guo, J.; Zhao, H.; Chai, D.; Zheng, X. *Appl. Catal., A* **2004**, *273*, 75−82.
(25) Qin, F.; Anderegg, J. W.; Jenks, C. J.; Gleeson, B.; Sordelet, D. J.; Thiel, P. A. *Surf. Sci.* **2008**, *602*, 205−215.
(26) Paryjczak, T.; Farbotko, J. M.; Jozwiak, K. W. *React. Kinet. Catal. Lett.* **1982**, *20*, 227−231.
(27) Schwartz, W. R.; Pfefferle, L. D. *J. Phys. Chem. C* **2012**, *116*, 8571−8578.
(28) Muller, C. A.; Maciejewski, M.; Koeppel, R. A.; Baiker, A. *Catal. Today* **1999**, *47*, 245−252.

DOI: 10.1021/acscatal.5b00060
ACS Catal. 2015, 5, 2916−2920